DNA-PKcs phosphorylation specific inhibitor, NU7441, enhances the radiosensitivity of clinically relevant radioresistant oral squamous cell carcinoma cells

KENTARO OHUCHI[1], RYO SAGA[2], KAZUKI HASEGAWA[2], EICHI TSURUGA[2], YOICHIRO HOSOKAWA[2], MANABU FUKUMOTO[3] and KAZUHIKO OKUMURA[1]

[1]Division of Reconstructive Surgery for Oral and Maxillofacial Region, Department of Human Biology and Pathophysiology, School of Dentistry, Health Sciences University of Hokkaido, Tobetsu-cho, Ishikari-gun, Hokkaido 061-0293; [2]Department of Radiation Science, Graduate School of Health Sciences, Hirosaki University, Hirosaki, Aomori 036-8564; [3]Pathology Informatics Team, RIKEN Center for Advanced Intelligence Project, Chuo-ku, Tokyo 103-0027, Japan

Received October 20, 2022; Accepted January 23, 2023

DOI: 10.3892/br.2023.1610

Abstract. Radioresistant cancer cells lead to poor prognosis after radiotherapy. However, the mechanisms underlying cancer cell radioresistance have not been fully elucidated. Thus, the DNA damage response of clinically relevant radioresistant oral squamous cell carcinoma HSC2-R cells, established by long-term exposure of parental HSC2 cells to fractionated radiation, was investigated. The DNA double-strand break (DSB) repair protein-specific inhibitor, NU7441, which targets DNA-dependent protein kinase catalytic subunit (DNA-PKcs) phosphorylation, and IBR2, which targets Rad51, were administered to HSC2 and HSC2-R cells. NU7441 administration eliminated colony formation in both cell lines under 6 Gy X-ray irradiation, whereas IBR2 did not affect colony formation. NU7441 and IBR2 significantly enhanced 6 Gy X-ray irradiation-induced apoptosis in HSC2-R cells. In HSC2-R cells, cell cycle arrest released earlier than in HSC2 cells, and phosphorylated-H2A histone family member X (γH2AX) expression rapidly decreased. Following NU7441 administration, γH2AX expression and the cell percentages of the G2/M phase were not decreased at 48 h after treatment in HSC2-R cells. DNA-PKcs has been demonstrated to regulate non-homologous end-joining (NHEJ) and homologous recombination (HR) repair, and the later phase of DSB repair is dominated by HR. Therefore, the results of the present study indicated that the DSB repair mechanism in HSC2-R cells strongly depends on NHEJ and loss of HR repair function. The present study revealed a potential mechanism underlying the acquired radioresistance and therapeutic targets in radioresistant cancer cells.

Correspondence to: Dr Ryo Saga, Department of Radiation Science, Graduate School of Health Sciences, Hirosaki University, 66-1 Hon-cho, Hirosaki, Aomori 036-8564, Japan
E-mail: sagar@hirosaki-u.ac.jp

Professor Kazuhiko Okumura, Division of Reconstructive Surgery for Oral and Maxillofacial Region, Department of Human Biology and Pathophysiology, School of Dentistry, Health Sciences University of Hokkaido, 1757 Kanazawa, Tobetsu-cho, Ishikari-gun, Hokkaido 061-0293, Japan
E-mail: kokumura@hoku-iryo-u.ac.jp

Key words: radioresistance, DNA damage response, NU7441, IBR2

Introduction

Current radiotherapy for tumors can achieve noninvasive local control, and plays an important role in cancer therapy (1). However, despite advances in irradiation technology, there are cases in which local control of the tumor fails and recurrence or metastasis occurs. From the viewpoint of radiation biology, cancer cells that exhibit intrinsic or extrinsic radioresistance during fractionated radiation therapy survive after treatment causing recurrence and metastasis (2). Elucidation of the mechanisms of radioresistance is an urgent issue for improving the outcomes of radiation therapy.

The major cell-killing effect of ionizing radiation is DNA damage [i.e., DNA double-strand breaks (DSBs)] caused by reactive oxygen species (ROS) (3,4). This lethal effect of ionizing radiation is modified by linear energy transfer, dose rate, oxygen concentration, cell cycle distribution, and the DNA damage response (DDR) of cells (5-9). In addition, the authors previously reported that an increase in the number of cancer stem cells (CSCs) among radioresistant cell lines is involved in the increase in cell survival following fractionated irradiation (i.e., sub-lethal damage repair) (10-12). DSB repair is completed mainly by non-homologous end joining (NHEJ) and homologous recombination (HR) (13). NHEJ is the dominant repair pathway throughout the cell cycle, and HR functions from the S phase to the M phase because it requires sister chromosomes (14). HR is frequently reported to be associated with radioresistance owing to error-free repair (15), whereas error-prone NHEJ has been reported to induce genome instability and allow radioresistant clones to expand (16). However, the detailed DNA repair pathway in radioresistant cancer cells remains unclear.

The radioresistant cell lines established after long-term exposure to fractionated irradiation exhibit clinically relevant radioresistance (17,18). It has been suggested that cancer cells acquire radioresistance during fractionated radiotherapy, resulting in poor prognosis. However, the mechanisms underlying radioresistance in cancer cells have not been fully clarified. Herein, to provide means of overcoming radioresistance, the differences in DDR between non-radioresistant and radioresistant cell lines using DSB repair protein-specific inhibitors were investigated, and may serve as a therapeutic target for eliminating radioresistant cancer cells in radiotherapy.

Materials and methods

Reagents. The DNA-dependent protein kinase (DNA-PK) inhibitor, NU7441, and the Rad51 inhibitor, IBR2, were purchased from Selleck Chemicals and MedChemExpress, respectively. These inhibitors were dissolved in 1 mM dimethyl sulfoxide (DMSO; i.e., 1.2092 ml for 5 mg NU7441 and 1.2485 ml for 5 mg IBR2; Sigma-Aldrich; Merck KGaA), administered at the indicated concentrations (i.e., 0.5, 1, 5 and 10 μM for NU7441; and 1, 5, 10 and 15 μM for IBR2) 1 h before irradiation, and then washed out using phosphate-buffered saline (PBS) without magnesium and calcium (Takara Bio, Inc.) 24 h after administration. Based on the pharmacokinetics that 80-90% of most anticancer drugs are excreted from the body within 24 h after administration (19), these were washed out after 24 h.

Cell culture. Human oral squamous carcinoma cell lines, HSC2 and HSC2-R, were used as models for non-radioresistant cells (HSC2) and radioresistant cells (HSC2-R). The HSC2 cell line (ID: TKG 0487) was provided by Cell Resource Center for Biomedical Research, Institute of Development, Aging and Cancer, Tohoku University (Sendai, Japan). HSC2-R cells were established by long-term exposure to fractionated irradiation (i.e., 2 Gy/day, over 60 Gy) (17). To confirm the origin of the HSC2 and HSC2-R cells, a short tandem repeat analysis was performed using a contract research service (BEX Co., Ltd.). The analysis revealed that both cell lines were the same as HSC2 cells registered at the National Institutes of Biomedical Innovation, Health and Nutrition (Osaka, Japan). These cell lines were maintained at 37˚C and 5% CO_2 in Roswell Park Memorial Institute 1640 medium (Thermo Fisher Scientific, Inc.) supplemented with 10% heat-inactivated fetal bovine serum (FBS; Japan Bio Serum) and 1% penicillin/streptomycin (Thermo Fisher Scientific, Inc.).

Irradiation. The cultured cells were irradiated using an X-ray generator (MBR-1520R-3; Hitachi, Ltd.) with 0.5-mm aluminum + 0.3-mm copper filters at a distance of 45 cm between the focus and target (150 kV, 20 mA, 1.0 Gy/min). During the X-ray exposure, the total dose and dose rate were monitored using a thimble ionization chamber placed next to the sample. The uncertainty in the absorbed dose measured by the thimble ionization chamber is ±1%.

Flow cytometric analysis. Apoptotic cells were detected using fluorescein isothiocyanate (FITC)-conjugated Annexin V (cat. no. 640906; BioLegend, Inc.) and propidium iodide (PI) (cat. no. 421301; BioLegend, Inc.). Trypsinized cells were adjusted to a density of $1x10^6$ cells/ml and washed with PBS without magnesium and calcium. Next, the cells were incubated for 20 min at 4˚C in the dark after the addition of FITC-Annexin V (5 μl/10^6 cells) and PI (10 μl/10^6 cells) and, analyzed by direct immunofluorescence flow cytometry using CytoFLEX (Beckman Coulter, Inc.). The percentage of FITC-Annexin V-positive cells was defined as the percentage of apoptotic cells i.e., FITC-Annexin V (+)/PI (-) fraction and FITC-Annexin V (+)/PI (+) fraction. To compensate for histone protein levels, the cell cycle distribution and phosphorylated-H2A histone family member X (γH2AX)-positive cells were measured using double staining (20). In particular, trypsinized cells were fixed with chilled 70% ethanol at -20˚C for 30 min, and then stained with PI (15 μl/10^6 cells) and FITC-γH2AX (5 μl/10^6 cells) in the presence of RNase (0.2 mg/ml, Nippon Gene Co., Ltd.) at room temperature in the dark for 15 min. The fluorescence data were analyzed using the CytExpert software ver. 2.4 (Beckman Coulter, Inc.). The concentrations of NU7441 and IBR2 used were 5 and 10 μM, respectively. The assessment time points were 1, 6, 24, and 48 h after 6 Gy irradiation in combination with NU7441 or IBR2 administration.

Colony formation assay. Clonogenic potency following treatment with 6 Gy irradiation and/or NU7441 or IBR2 administration was evaluated using a colony formation assay. For the non-irradiated and irradiated group, 400 and 10,000 cells were seeded on φ60 cell culture dishes, respectively. After 6 h of incubation at 37˚C, to allow the cells to adhere to the bottom of the dish, NU7441 or IBR2 was administered. Subsequently, 1 h after administration, the cells were irradiated. After 24 h of administration, NU7441 or IBR2 were washed out with PBS and cells were cultured for an 7-10 additional days. The cells were then fixed with methanol (Wako Pure Chemical Industries, Ltd.) for 1 min and stained with Giemsa staining solution (Wako Pure Chemical Industries) for 2 h. These aforementioned procedures were performed at room temperature. Colonies with >50 cells were counted manually. The surviving fraction for each cell line was calculated from the ratio of the plating efficiency of the irradiated cells to that of the untreated group.

Statistical analysis. The significance of the differences between the control and experimental cultures was determined using the Tukey-Kramer post hoc test after one-way analysis of variance. Statistical analyses were performed using Microsoft Excel 2010 (Microsoft Corporation) with the add-on software Statcel v3 (OMS Publishing). The data shown in this manuscript were obtained by repeating the experiments thrice, and are presented as the mean ± SD. $P<0.05$ was considered to indicate a statistically significant difference.

Results

Cytotoxicity of NU7441 and IBR2. To investigate NU7441 and IBR2 toxicity in HSC2 and HSC2-R cells, the surviving cell fraction at 0.5, 1, 5, and 10 μM for NU7441 and 1, 5, 10, and 15 μM for IBR2 was measured using a colony formation

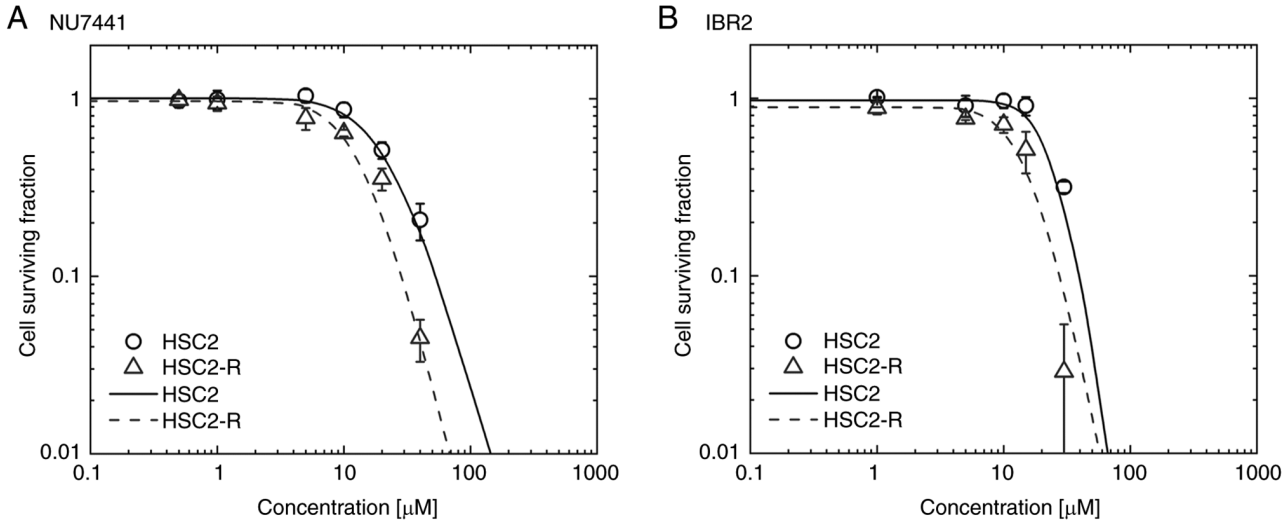

Figure 1. Cytotoxicity of NU7441 and IBR2. The cell surviving fraction after administration of (A) NU7441 and (B) IBR2 was assessed by colony formation assay. The circles with solid lines and the triangles with broken lines show the experimental and calculated cell survival of HSC2 and HSC2-R cells, respectively.

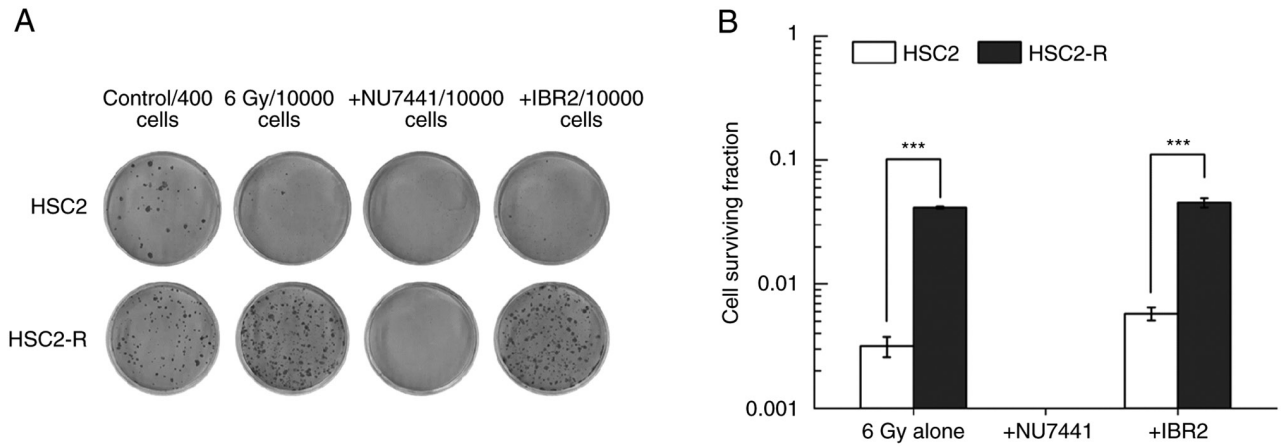

Figure 2. Radiosensitizing effects of NU7441 and IBR2. (A) Representative colony image with the number of seeded cells and (B) calculated cell survival fraction. Values are presented as the mean ± standard deviation. ***P<0.001.

assay. The surviving cell fraction was fitted using log logistic regression, and the 50% inhibitory dose (IC_{50}) was calculated. Following NU7441 administration, the cell surviving fraction of HSC2 and HSC2-R cells was decreased at 10 μM (Fig. 1A), and the IC_{50} was 21.21 μM for HSC2 and 13.44 μM for HSC2-R cells indicating HSC2-R cells were more sensitive to NU7441 than HSC2 cells (Fig. 1A). Following IBR2 administration, the surviving fraction decreased at 20 μM for HSC2 cells and 10 μM for HSC2-R cells (Fig. 1B). The IC_{50} value indicating sensitivity to IBR2 was 25.75 μM for HSC2 cells and 15.59 μM for HSC2-R cells. Radioresistant HSC2-R cells were more sensitive to both the DNA-PKcs inhibitor, NU7441, and the Rad51 inhibitor, IBR2, than non-radioresistant HSC2 cells.

The radiosensitization effects of NU7441 and IBR2. The surviving cell fraction following treatment with a combination of 6 Gy irradiation and NU7441 or IBR2 was measured using a colony formation assay. Both inhibitors, NU7441 and IBR2, were used at concentrations that did not reduce or slightly affect cell survival (i.e., 5 μM for NU7441 and 10 μM for IBR2). The surviving fraction of radioresistant HSC2-R cells was significantly higher than that of non-radioresistant HSC2 cells following treatment with 6 Gy irradiation alone (4.14±0.08% vs. 0.32±0.06%) (Fig. 2A and B). Although HSC2 and HSC2-R cells did not exhibit decreased cell survival after administration of 5 μM NU7441 alone (Fig. 1A), no countable colonies were observed following combination treatment with 6 Gy irradiation and NU7441 (Fig. 2A). There was no significant difference between 6 Gy irradiation alone and the combination of 6 Gy irradiation and IBR2 administration in either cell line.

Apoptosis induction under radiation combined with NU7441 or IBR2. The percentage of apoptotic cells was assessed after 24 and 48 h of treatment using Annexin V and PI staining. Apoptotic cells were defined as Annexin V-positive cells [i.e., Annexin V (+)/PI (-) and Annexin V (+)/PI (+) fractions] (Fig. 3A and B). The percentage of apoptotic HSC2-R cells

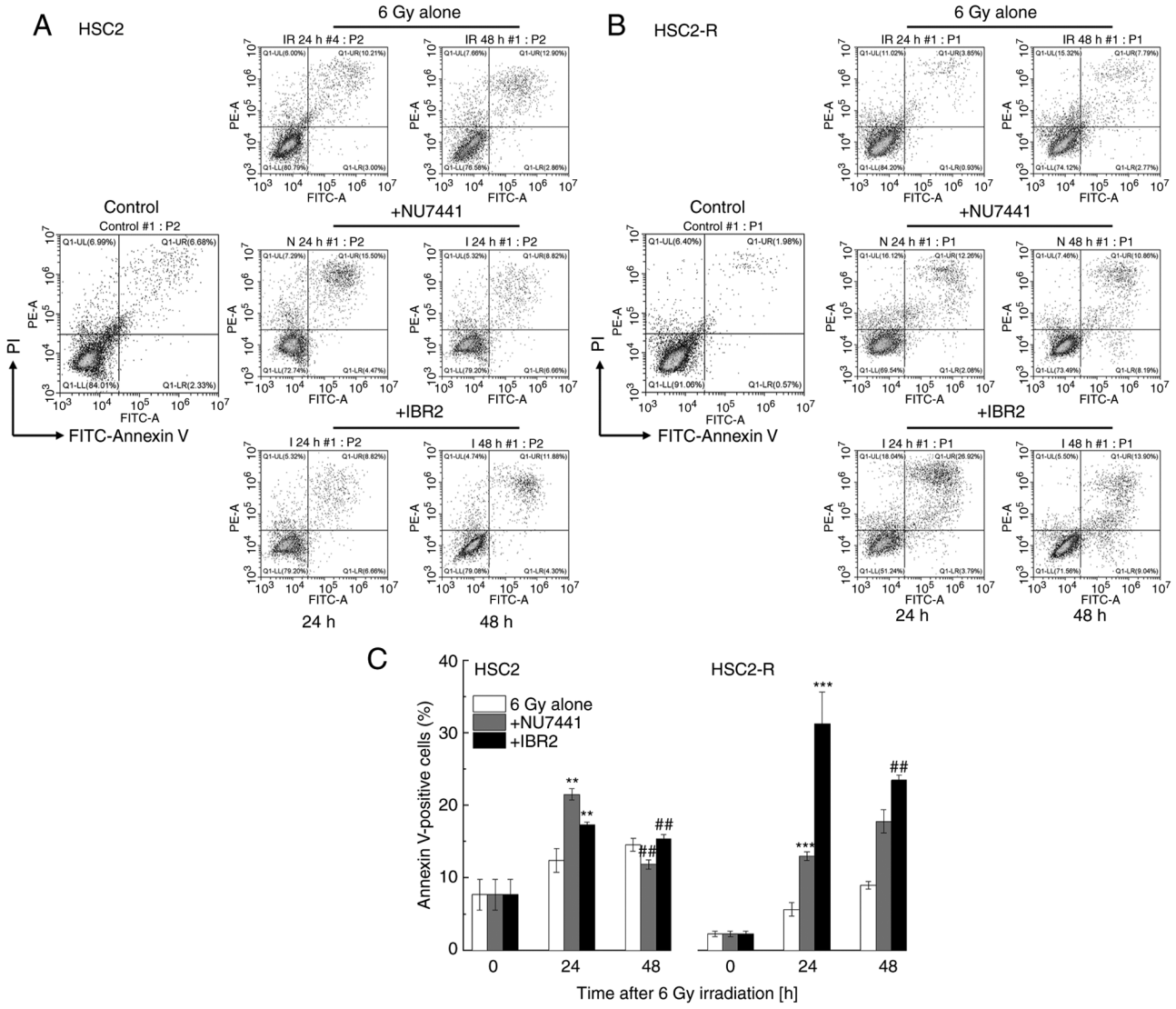

Figure 3. Percentage of apoptotic cells in non-radioresistant and radioresistant cells. (A and B) Representative dot plots of HSC2 and HSC2-R cells at 24 and 48 h after 6 Gy irradiation alone, or in combination with NU7441 or IBR2. (C) Quantitative analysis of apoptotic cell fractions, which was defined as FITC-Annexin V-positive cell fractions i.e., FITC-Annexin V (+)/PI (-) fraction and FITC-Annexin V (+)/PI (-) at 24 and 48 h after treatment. Values are presented as the mean ± standard deviation. **P<0.01 and ***P<0.001 vs. the same treatment group at 0 h; $^{\#\#}$P<0.01 vs. the same treatment group at 24 h. FITC, fluorescein isothiocyanate; PI, propidium iodide.

24 h after treatment with 6 Gy irradiation alone was significantly lower than that of apoptotic HSC2 cells (5.66±0.93% vs. 12.38±1.64%, respectively) (Fig. 3C). At 48 h after 6 Gy irradiation, the percentage of apoptotic HSC2-R cells significantly increased compared to that at 24 h after treatment with irradiation (8.98±0.50%) but was lower than that of apoptotic HSC2 cells (14.55±0.88%). Following treatment with the combination of radiation and NU7441, the percentage of apoptotic HSC2 cells was significantly increased (21.52±0.76%) compared to that of HSC2-R cells (13.02±0.61%) at 24 h. At 48 h after treatment, the percentage of apoptotic HSC2 cells was then decreased (11.86±0.64%), and that of HSC2-R cells was further increased (17.77±1.61%). Meanwhile, IBR2 treatment for 24 h induced more apoptosis in HSC2-R cells (31.29±4.36%) than in HSC2 cells (17.32±0.37%), and then decreased at 48 h (15.35±0.59% for HSC2 cells; 23.48±0.67% for HSC2-R cells) (Fig. 3C). Although the radioresistant HSC2-R cells were apoptosis-resistant compared with HSC2 cells, both inhibitors significantly induced apoptosis at least at 24 h.

DNA damage response following administration of NU7441 or IBR2 in combination with 6 Gy irradiation. To compensate for the amount of histone protein that depends on DNA content, the cell cycle distribution of cells and γH2AX dynamics were assessed concurrently using flow cytometry. The measurement time points were 1, 6, 24, and 48 h after 6 Gy irradiation in combination with NU7441 or IBR2 administration (Fig. 4). The cell cycle distribution-dependent γH2AX-positive fraction was observed 48 h after treatment, and the G2/M phase fraction was found to be decreased, especially in the 6 Gy + NU7441 group (Fig. 4A and B). The number of γH2AX-positive HSC2 and HSC2-R cells increased at 1 h after treatment and then, it was rapidly decreased after 6 h of treatment in the 6 Gy alone group and the 6 Gy + IBR2 group, but not in the 6 Gy + NU7441 group (Fig. 4C). At 24-48 h of treatment with 6 Gy

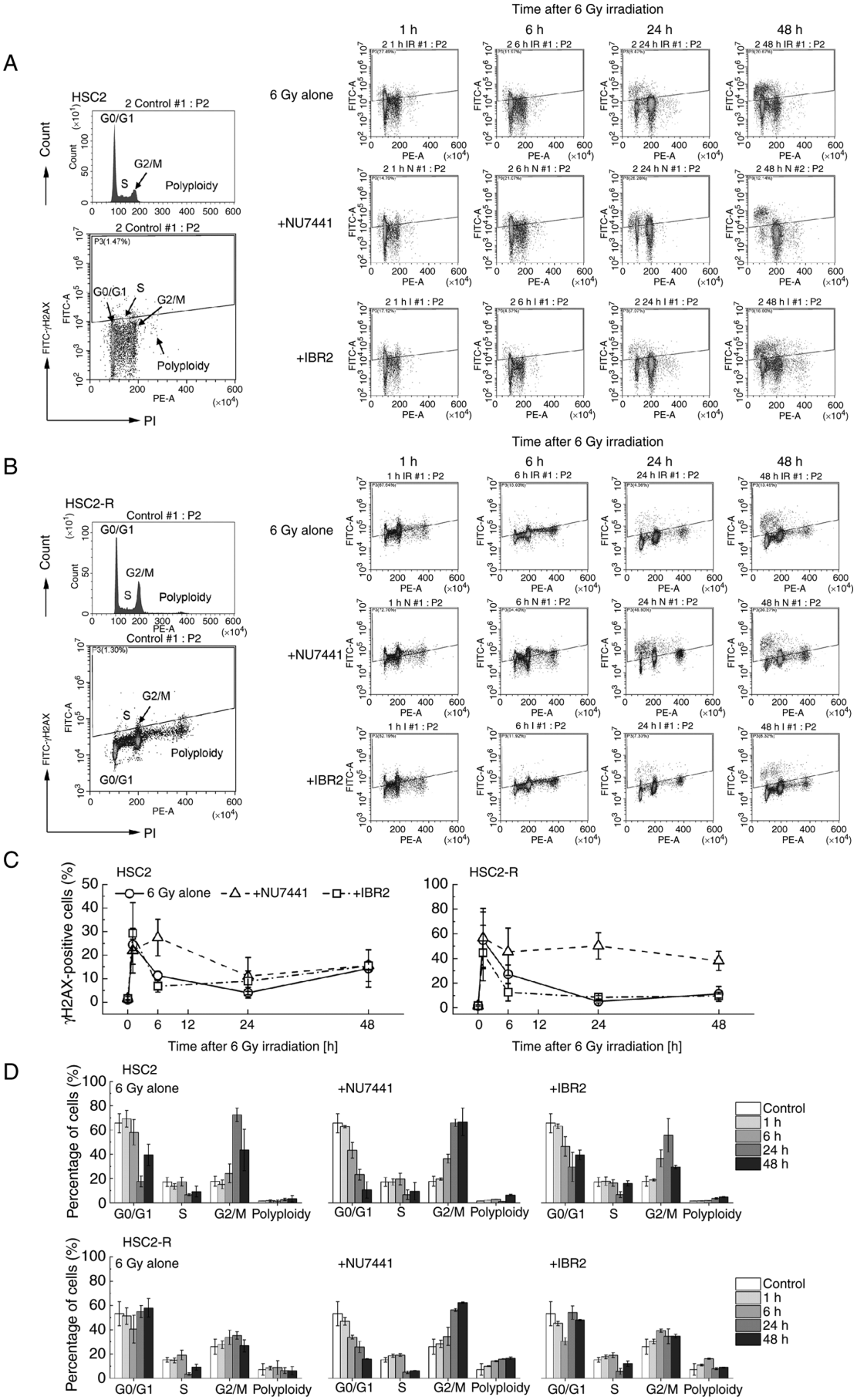

Figure 4. Cell cycle distribution and γH2AX dynamics after 6 Gy irradiation and/or combination with NU7441 or IBR2 administration. Representative dot plots and histograms of (A) HSC2 and (B) HSC2-R cells. (C) Fraction of γH2AX-positive cells and (D) cell populations in each cell cycle phase. Values are presented as the mean ± standard deviation. γH2AX, phosphorylated-H2A histone family member X.

irradiation alone or in combination with IBR2, the number of γH2AX-positive HSC2 cells gradually increased, whereas that of HSC2-R cells did not change. Upon NU7441 administration, the number of γH2AX-positive HSC2 cells began to decrease between 6 and 24 h, and then gradually increased until 48 h. Meanwhile, the number of γH2AX-positive HSC2-R cells slightly decreased at 6 h compared with that at 1 h, but remained high compared to the 6 Gy alone and 6 Gy + IBR2 groups at 24 to 48 h.

The cell cycle distribution of HSC2 cells after 6 Gy irradiation did not change until 6 h. At 24 h, the percentage of cells in the G2/M phase was markedly higher than that at 0, 1, and 6 h, while the percentage of cells in the G0/G1 and S phases decreased at this time point, suggesting that cells were arrested at the G2/M checkpoint (Fig. 4D). At 48 h, this arrest tended to be released. The kinetics of the cell cycle distribution were the same as those of the 6 Gy + IBR2 group. Meanwhile, in the 6 Gy + IBR2 treatment group of HSC2-R cells, the cells in the G0/G1 phase were decreased and the cells in the G2/M phase were slightly increased at the 6-h time point, and then arrest was released after 24 h (Fig. 4D). In the 6 Gy + NU7441 group, the number of cells in the G0/G1 phase decreased continuously 1 h after treatment in both cell lines, while the G2/M phase cell population increased. NU7441 combined with 6 Gy irradiation extended G2/M arrest. Notably, in HSC2-R cells, polyploid cell populations were more abundant than in HSC2 cells and increased over time following NU7441 administration.

Discussion

In the present study, the DDR of radioresistant HSC2-R cells and the non-radioresistant parental HSC2 cells was investigated using the DNA-PKcs inhibitor, NU7441, and Rad51 inhibitor, IBR2. DNA-PKcs is a major NHEJ protein, whereas Rad51 is a major HR protein (21,22). Both DNA repair mechanisms are important in radiation-induced lethal DSBs. In the present study, it was determined that radioresistant HSC2-R cells were more sensitive to both DNA repair inhibitors than non-radioresistant HSC2 cells, as indicated by the corresponding IC_{50} values (Fig. 1). In addition, the combination of NU7441 administration and 6 Gy irradiation eliminated colony formation in HSC2 and HSC2-R cells, whereas IBR2 administration with 6 Gy irradiation did not affect colony formation after 24 h of exposure. Because exposure to both inhibitors for >24 h completely eliminated colony formation, cell survival at other experimental time points was not feasible.

It has been reported that oral squamous cell carcinoma cell lines such as SAS and HSC4 are HR deficient (23). There are no reports on the HR capacity of HSC2 and HSC2-R cells, but the lack of colony formation inhibitory effects of IBR2 administration with 6 Gy irradiation suggests that it may not be very proficient. In addition, long-term exposure of HepG2 and HeLa cells to fractionated radiation was revealed to increase the protein levels of phosphorylated DNA-PKcs (24). Based on these findings, the main DNA repair pathway in radioresistant HSC2-R cells is suggested to be NHEJ. By contrast, a nasopharyngeal carcinoma cell line exhibited increased levels of HR-associated repair proteins RPA1, BRCA2, BRCA1, and Rad51 after long-term exposure to fractionated irradiation (25). These differences are thought to depend on the phenotype of the parental cell line; however, alternative epigenetic repair mechanisms may be induced by genomic instability (26). Indeed, HepG2 cells that acquired radioresistance had a high mutation frequency at the *hypoxanthine phosphoribosyltransferase* locus compared to parental cells (27). It should be noted that genome instability is also induced by error-prone backup DSB repair mechanisms, that is, alternative-end joining and single-strand annealing (28), but its association with radioresistance of cells has not yet been reported.

The apoptotic fraction of HSC2-R cells following 6 Gy irradiation was lower than that of HSC2 cells, and both NU7441 and IBR2 significantly promoted apoptosis in both cell lines 24 h after administration (Fig. 3). Several studies have reported the induction of apoptosis by the combined use of Rad51 inhibitor and other cytotoxic agents. B02, a RAD51-targeting agent, synergistically increased cytotoxicity stimulated by doxorubicin (29) or AZD1775 (30). In addition, Rad51 inhibition enhanced radiation-induced cell death (31,32). In HSC2 cells, the apoptotic fraction decreased at 48 h after administration of both inhibitors compared with that at 24 h, and this phenomenon was observed only after IBR2 administration in HSC2-R cells. According to recent views, apoptosis is reversible, a process referred to as anastasis, and caspases outside of apoptosis promote tumor repopulation (33). Therefore, the decrease in apoptotic cell fraction may be due to anastasis. Most anticancer agents are excreted from the human body within 24 h. Based on the pharmacokinetics, the inhibitors were washed out after 24 h. Such experimental manipulations may also affect the fraction of apoptotic cells. In addition, exposure to inhibitors was only performed for 24 h in the experiment of the present study. Both inhibitors should be investigated at further experimental time points in the future. A further limitation of the present study, was that the apoptotic cell fraction under the treatment of NU7441 or IBR2 without 6 Gy irradiation was not confirmed. The apoptotic effects of NU7441 and IBR2 could modify the cell surviving fraction; however, the colony formation was not significantly decreased at the concentration used in the present study (Fig. 1). Regarding the concentration i.e., 5 μM NU7441 and 10 μM IBR2 used, previous studies have reported that these concentrations do not significantly induce apoptosis (34,35).

The cell cycle distribution and γH2AX dynamics of HSC2 and HSC2-R cells was assessed by flow cytometric analysis. The γH2AX-positive fraction of HSC2 and HSC2-R cells was increased 1 h after treatment, and then immediately reduced (i.e., 6 h after treatment) (Fig. 4). Only NU7441 administration maintained the size of the fractions, suggesting that NHEJ was predominant in the early phase of the repair process. Strong G2/M phase arrest was observed following NU7441 administration in HSC2 and HSC2-R cells. Although HSC2 cells exhibited reduced γH2AX-positive fractions, those of γH2AX-positive HSC2-R cells remained high from 24 to 48 h. Following IBR2 administration in HSC2-R cells, cell cycle distribution and γH2AX expression was not significantly altered compared with the treatment with 6 Gy irradiation alone (Fig. 4C and D). The percentage of γH2AX-positive HSC2 cells increased again at 48 h, but not that of HSC2-R cells. HR is the predominant

repair pathway at the later phase of the repair process that causes secondary replication-induced DSBs (36). It has been reported that DNA-PKcs can regulate the selection of the DSB repair pathway according to the cell cycle phase. In the S and G2 phases of the cell cycle, DNA-PKcs dissociation from DSBs by autophosphorylation results in the selection of the HR repair pathway to promote the end resection of DSB sites (37,38). In addition, inducing HR deletions results in greater radioresistance compared to the parental cell line (39), and restoring the HR mechanism in HR-deficient cancers renders them radiosensitive (40). These observations and studies suggest that the repair mechanism of HSC2-R cells strongly depends on DNA-PKcs phosphorylation, and a weak repair mechanism during the S and G2/M phases. In the present study, the protein expression of DDR signaling pathways including targets of NU7441 or IBR2, was not investigated. The protein expression related to cell cycle regulation and DNA repair should be investigated in the future. Furthermore, the potential radioresistance mechanisms in HSC2-R cells may be associated with an increase in the polyploidy fraction. It has been reported that the majority of polyploid giant cancer cells (PGCCs), induced by irradiation, undergo cell death, but some PGCCs exhibit proliferative capacity and undergo neosis, which may result in tumor repopulation (41). NU7441 and IBR2 increased the polyploid fraction in HSC2-R cells. However, the fate of the polyploid fraction of cells requires long-term observation; therefore, this population needs to be tracked further in the future.

In the present study, using inhibitors targeting two major DSB repair proteins, the mechanism of radioresistance acquisition and targets for overcoming radioresistance of cells were revealed. The DNA-PKcs specific inhibitor, NU7441, markedly decreased colony formation in radioresistant HSC2-R cells by suppressing DDR in the S and G2/M phases. Meanwhile, the Rad51 specific inhibitor, IBR2, promoted apoptosis in radioresistant HSC2-R cells, but colony formation and DDR were not altered compared to 6 Gy irradiation alone, suggesting that HR may not be the primary DSB repair pathway in HSC2-R cells. Based on the findings of the present study, the DSB repair pathway of radioresistant cells depends on NHEJ. Therefore, it is suggested that targeting DNA-PKcs aids in eliminating radioresistant cancer cells, and thus overcoming treatment resistance and preventing recurrence. However, the detailed molecular pathways underlying this mechanism should be studied in the future.

Acknowledgements

We would like to thank Dr Tomita (Kagoshima University, Kagoshima, Japan) and Dr Kuwahara (Tohoku Medical and Pharmaceutical University, Sendai, Japan) for donating the radioresistant cells.

Funding

Funding was provided by Japan Society for the Promotion of Science (grant nos. 20K16814 and 19K08141). The funders had no role in the study design, data collection and analysis, decision to publish, or preparation of the manuscript.

Availability of data and materials

The datasets used and/or analyzed during the current study are available from the corresponding author on reasonable request.

Authors' contributions

KOh and RS conceived the study, participated in its design and coordination, and drafted the manuscript. KOh, RS and KH participated in the experiments, and performed the analysis and interpretation of the data. ET, YH, MF and KOk critically reviewed the article for important intellectual content. KH, ET, YH, MF and KOk confirm the authenticity of all the raw data. All authors read and approved the final manuscript.

Ethics approval and consent to participate

Not applicable.

Patient consent for publication

Not applicable.

Competing interests

The authors declare that they have no competing interests.

References

1. Atun R, Jaffray DA, Barton MB, Bray F, Baumann M, Vikram B, Hanna TP, Knaul FM, Lievens Y, Lui TY, *et al*: Expanding global access to radiotherapy. Lancet Oncol 16: 1153-1186, 2015.
2. Olivares-Urbano MA, Griñán-Lisón C, Marchal JA and Núñez MI: CSC Radioresistance: A therapeutic challenge to improve radiotherapy effectiveness in cancer. Cells 9: 1651, 2020.
3. Bajinskis A, Natarajan AT, Erixon K and Harms-Ringdahl M: DNA double strand breaks induced by the indirect effect of radiation are more efficiently repaired by non-homologous end joining compared to homologous recombination repair. Mutat Res 756: 21-29, 2013.
4. Vignard J, Mirey G and Salles B: Ionizing-radiation induced DNA double strand breaks: A direct and indirect lighting up. Radiother Oncol 108: 362-369, 2013.
5. Hawkins RB and Inaniwa T: A microdosimetric-kinetic model for cell killing by protracted continuous irradiation including dependence on LET I: Repair in cultured mammalian cells. Radiat Res 180: 584-594, 2013.
6. Matsuya Y, McMahon SJ, Tsutsumi K, Sasaki K, Okuyama G, Yoshii Y, Mori R, Oikawa J, Prise KM and Date H: Investigation of dose-rate effects and cell-cycle distribution under protracted exposure to ionizing radiation for various dose-rates. Sci Rep 8: 8287, 2018.
7. Qi XS, Pajonk F, McCloskey S, Low DA, Kupelian P, Steinberg M and Sheng K: Radioresistance of the breast tumor is highly correlated to its level of cancer stem cell and its clinical implication for breast irradiation. Radiother Oncol 124: 455-461, 2017.
8. Matsuya Y, McMahon SJ, Butterworth KT, Naijo S, Nara I, Yachi Y, Saga R, Ishikawa M, Sato T, Date H and Prise KM: Oxygen enhancement ratios of cancer cells after exposure to intensity modulated X-ray fields: DNA damage and cell survival. Phys Med Biol 66 2021.
9. Kim RK, Suh Y, Cui YH, Hwang E, Lim EJ, Yoo KC, Lee GH, Yi JM, Kang SG and Lee SJ: Fractionated radiation-induced nitric oxide promotes expansion of glioma stem-like cells. Cancer Sci 104: 1172-1177, 2013.
10. Fukui R, Saga R, Matsuya Y, Tomita K, Kuwahara Y, Ohuchi K, Sato T, Okumura K, Date H, Fukumoto M and Hosokawa Y: Tumor radioresistance caused by radiation-induced changes of stem-like cell content and sub-lethal damage repair capability. Sci Rep 12: 1056, 2022.

11. Saga R, Matsuya Y, Takahashi R, Hasegawa K, Date H and Hosokawa Y: Analysis of the high-dose-range radioresistance of prostate cancer cells, including cancer stem calls, based on a stochastic model. J Radiat Res 60: 298-307, 2019.
12. Murata K, Saga R, Monzen S, Tsuruga E, Hasegawa K and Hosokawa Y: Understanding the mechanism underlying the acquisition of radioresistance in human prostate cancer cells. Oncol Lett 17: 5830-5838, 2019.
13. Shibata A: Regulation of repair pathway choice at two-ended DNA double-strand breaks. Mutat Res 803-805: 51-55, 2017.
14. Shibata A and Jeggo PA: DNA double-stand break repair in a cellular context. Clin Oncol (R Coll Radiol) 26: 243-249, 2014.
15. Karanam K, Kafri R, Loewer A and Lahav G: Quantitative live cell imaging reveals a gradual shift between DNA repair mechanisms and a maximal use of HR in mid S phase. Mol Cell 47: 320-329, 2012.
16. Wang Y, Xu H, Liu T, Huang M, Butter PP, Li C, Zhang L, Kao GD, Gong Y, Maity A, *et al*: Temporal DNA-PK activation drives genomic instability and therapy resistance in glioma stem cells. JCI insight 3: e98096, 2018.
17. Kuwahara Y, Mori M, Oikawa T, Shimura T, Ohtake Y, Mori S, Ohkubo Y and Fukumoto M: The modified high-density survival assay is the useful tool to predict the effectiveness of fractionated radiation exposure. J Radiat Res 51: 297-302, 2010.
18. Kuwahara Y, Roudkenar MH, Urushihara Y, Saito Y, Tomita K, Roushandeh AM, Sato T, Kurimasa A and Fukumoto M: Clinically relevant radioresistant cell line: A simple model to understand cancer radioresistance. Med Mol Morphol 50: 195-204, 2017.
19. Liston DR and Davis M: Clinically relevant concentrations of anticancer drugs: A guide for nonclinical studies. Clin Cancer Res 23: 3489-3498, 2017.
20. Huang X, Okafuji M, Traganos F, Luther E, Holden E and Darzynkiewicz Z: Assessment of histone H2AX phosphorylation induced by DNA topoisomerase I and II inhibitors topotecan and mitoxantrone and by the DNA corss-linking agent cisplatin. Cytometry A 58: 99-110, 2004.
21. Difilippantonio MJ, Zhu J, Chen HT, Meffre E, Nussenzweig MC, Max EE, Ried T and Nussenzweig A: DNA repair protein Ku80 suppresses chromosomal aberrations and malignant transformation. Nature 404: 510-514, 2000.
22. Tachon G, Cortes U, Guichet PO, Rivet P, Balbous A, Masliantsev K, Berger A, Boissonnade O, Wager M and Karayan-Tapon L: Cell cycle changes after glioblastoma stem cell irradiation: The major role of RAD51. Int J Mol Sci 19: 3018, 2018.
23. Wurster S, Hennes F, Parplys AC, Seelbach JI, Mansour WY, Zielinski A, Petersen C, Clauditz TS, Münscher A, Friedl AA and Borgmann K: PARP1 inhibition radiosensitizes HNSCC cells deficient in homologous recombination by disabling the DNA replication fork elongation response. Oncotarget 7: 9732-9741, 2016.
24. Shimura T, Kakuda S, Ochiai Y, Nakagawa H, Kuwahara Y, Takai Y, Kobayashi J, Komatsu K and Fukumoto M: Acquired radioresistance of human tumor cells by DNA-PK/AKT/GSK3beta-mediated cyclin D1 overexpression. Oncogene 29: 4826-4837, 2010.
25. Wang Z, Zuo W, Zeng Q, Li Y, Lu T, Bu Y and Hu G: The homologous recombination repair pathway is associated with resistance to radiotherapy in nasopharyngeal carcinoma. Int J Biol Sci 16: 408-419, 2020.
26. Bakhoum SF and Cantley LC: The multifaceted role of chromosomal instability in cancer and its microenvironment. Cell 174: 1347-1360, 2018.
27. Kuwahara Y, Roudkenar MH, Urushihara Y, Saito Y, Tomita K, Roushandeh AM, Sato T, Kurimasa A and Fukumoto M: X-ray induced mutation frequency at the Hypoxanthine Phosphoribosyltransferase locus in clinically relevant radioresistant cells. Int J Med Phs Clin Eng Radiat Oncol 6: 377-391, 2017.
28. Ceccaldi R, Rondinelli B and D'Andrea AD: Repair pathway choices and consequences at the double-strand break. Trends Cell Biol 26: 52-64, 2016.
29. Schurmann L, Schumacher L, Roquette K, Brozovic A and Fritz G: Inhibition of the DSB repair protein RAD51 potentiates the cytotoxic efficacy of doxorubicin via promoting apoptosis-related death pathways. Cancer Lett 520: 361-373, 2021.
30. Lindemann A, Patel AA, Tang L, Tanaka N, Gleber-Netto FO, Bartels MD, Wang L, McGrail DJ, Lin SY, Frank SJ, *et al*: Combined Inhibition of Rad51 and wee1 enhances cell killing in HNSCC through induction of apoptosis associated with excessive DNA damage and replication stress. Mol Cancer Ther 20: 1257-1269, 2021.
31. Sak A, Stueben G, Groneberg M, Bocker W and Struschke M: Targeting of Rad51-dependent homologous recombination: Implications for the radiation sensitivity of human lung cancer cell lines. Br J Cancer 92: 1089-1097, 2005.
32. Wéra AC, Lobbens A, Stoyanov M, Lucas S and Michiels C: Radiation-induced synthetic lethality: Combination of poly(ADP-ribose) polymerase and RAD51 inhibitors to sensitize cells to proton irradiation. Cell Cycle 18: 1770-1783, 2019.
33. Mirzayans R and Murray D: Intratumor heterogeneity and therapy resistance: Contributions of dormancy, apoptosis reversal (anastasis) and cell fusion to disease recurrence. Int J Mol Sci 21: 1308, 2020.
34. Yanai M, Makino H, Ping B, Takeda K, Tanaka N, Sakamoto T, Yamaguchi K, Kodani M, Yamasaki A, Igishi T and Shimizu E: DNA-PK inhibition by NU7441 enhances chemosensitivity to topoisomerase inhibitor in non-small cell lung carcinoma cells by blocking DNA damage repair. Yonago Acta Med 60: 9-15, 2017.
35. Zhu J, Zhou L, Wu G, Konig H, Lin X, Li G, Qiu XL, Chen CF, Hu CM, Goldblatt E, *et al*: A novel small molecule RAD51 inactivator overcomes imatinib-resistance in chronic myeloid leukaemia. EMBO Mol Med 5: 353-365, 2013.
36. Groth P, Orta ML, Elvers I, Majumder MM, Lagerqvist A and Helleday T: Homologous recombination repairs secondary replication induced DNA double-strand breaks after ionizing radiation. Nucleic Acids Res 40: 6585-6594, 2012.
37. Yue X, Bai C, XieD, Ma T and Zhou PK: DNA-PKcs: A multi-faceted player in DNA damage response. Front Genet 11: 607428, 2020.
38. Shibata A, Conrad S, Birraux J, Geuting V, Barton O, Ismail A, Kakarougkas A, Meek K, Taucher-Scholz G, Löbrich M and Jeggo PA: Factors determining DNA double-strand break repair pathway choice in G2 phase. EMBO J 30: 1079-1092, 2011.
39. Frankenberg-Schwager M, Gebauer A, Koppe C, Wolf H, Pralle E and Frankenberg D: Single-strand annealing, conservative homologous recombination, nonhomologous DNA end joining, and the cell cycle-dependent repair of DNA double-strand breaks induced by sparsely or densely ionizing radiation. Radiat Res 171: 265-273, 2009.
40. Barazas M, Gasparini A, Huang Y, Küçükosmanoğlu A, Annunziato S, Bouwman P, Sol W, Kersbergen A, Proost N, de Korte-Grimmerink R, *et al*: Radiosensitivity is an acquired vulnerability of PARPi-resistant BRCA1-deficient tumors. Cancer Res 79: 452-460, 2019.
41. Zhang Z, Feng X, Deng Z, Chen J, Wang Y, Zhao M, Zhao Y, He S and Huang Q: Irradiation-induced polyploid giant cancer cells are involved in tumor cell repopulation via neosis. Mol Oncol 15: 2219-2234, 2021.